Pattern Genomic Probes Inside Capillary Tubes by Magneto Lithography Method Producing Parallel Detection of DNA and RNA

Amos Bardea[1,2][a]
[1]Holon Institute of Technology (HIT), Golomv Street, Holon, Israel
[2]Faculty of Engineering, Holon Institute of Technology (HIT), Israel

Keywords: Lithography, Patterning, DNA Sensors, Parallel Sensing.

Abstract: Here we present a new technique that introduces the possibility to pattern inside closed volume using the Magneto lithography (ML) method which allows the chemical patterning of the inside of the micro-channel tube. The ML method is a bottom-up method but at the same time, it provides the desired high-throughput capabilities for mass production. The ML method simplifies chemical surface patterning because it does not require resist, which may contaminate the substrate. ML can also be applied for applications combining both microelectronics and chemical patterning. Furthermore, ML does not depend on the surface topography and planarity, and can pattern non-flat surfaces and the inside surfaces of a closed volume, therefore, ML allows the chemical patterning of the inside of tubes.

1 INTRODUCTION

Magneto lithography (ML) is based on ‘‘patterning’’ a magnetic field on a substrate by applying a constant magnet and using paramagnetic metal masks that define the spatial distribution and shape of the applied field. The second component in ML is ferromagnetic nanoparticles that are assembled onto the substrate according to the field induced by the mask. Similar to Photolithography (Pease 2008), ML can be used to apply either a positive or negative mode. In the positive mode, the magnetic nanoparticles react chemically or interact via chemical recognition with the substrate. Hence, the magnetic nanoparticles are immobilized at selected locations, where the mask induces a magnetic field, resulting in a patterned substrate. In the negative mode, the magnetic nanoparticles do not interact chemically with the substrate. Hence, once they pattern the substrate, they block their site on the substrate. The exposed areas, not covered by the nanoparticles, can at this stage, be covered by molecules that chemically bind to the substrate. After the binding of these molecules, the nanoparticles are removed, resulting in a “negatively” patterned substrate. We introduced the ML method, in which a paramagnetic mask is applied for patterning of surfaces with high throughput (Ito, 2000, Service 2001, Hoeppener 2003, Stewart 2007, De Marco 2008). It can be easily applied for chemical patterning surfaces (Li, 2003, McClelland 2002) and for common microelectronic processes such as etching and deposition with various magnetic masks, permanent, dynamic and hard disk masks (Bandic 2003, Urbach 2003, Bardea 2009, Bardea 2017, Bardea 2018). Here, we show the capabilities of ML for patterning the inside of tubes by demonstrating positive and negative ML processes and sequential reactions made possible by these processes.

2 METHODOLOGY AND RESULTS

As previously mentioned, the ability to apply the ML method does not depend on the surface topography and planarity; therefore, ML allows the chemical patterning of the inside of tubes. The ML can pattern the inside of tubes by applying either positive or negative routes. Figure 1 shows the positive ML process for patterning the surface of inner tubes (100-µm inner diameter). The inner surface of a glass tube was functionalized with mercaptosilane. Ten-

[a] https://orcid.org/0000-0002-0512-4120

Bardea, A.
Pattern Genomic Probes Inside Capillary Tubes by Magneto Lithography Method Producing Parallel Detection of DNA and RNA.
DOI: 10.5220/0011872000003414
In *Proceedings of the 16th International Joint Conference on Biomedical Engineering Systems and Technologies (BIOSTEC 2023) - Volume 1: BIODEVICES*, pages 80-84
ISBN: 978-989-758-631-6; ISSN: 2184-4305

nanometer-diameter magnetic nanoparticles (Fe_3O_4) were coated by fluorescein and sulforhodamine. A magnetic field was applied on the tube by using a permanent magnet. The fluorescein-labeled magnetic nanoparticles were injected into the tube and adsorbed at those sites where the magnetic field gradient was maximal. Thereafter the tube was washed with ethanol and the magnet field was shifted to another site. Next, sulforhodamine-labeled magnetic nanoparticles were injected into the tube and they concentrated at the new site. This process resulted in two fluorescence bands and profile of the fluorescence signal as shown in Figure 1.

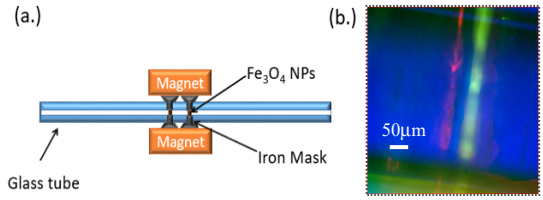

Figure 1: (a) A scheme describing the patterning of the inner tube surface by applying positive ML. (b) The fluorescence of both fluorescein and sulforhodamine observed from the two bands of the nanoparticles adsorbed within the tube.

In the ML process, we expose a substrate whose surface is patterned by a magnetic field, to magnetic NPs. The force applied on the magnetic NPs is given by:

$$\mathbf{F}=\Delta\chi V(\nabla\cdot\boldsymbol{B})\boldsymbol{B}\mu_0^{-1} \quad (1)$$

where B is the magnetic flux density (Tesla), $\Delta\chi$ is the difference in susceptibility between an object and its surroundings (10^3-10^5 m^{-3} for paramagnetic materials in air), V is the volume (~$1x10^{-19}$ cm^3 for a 10-nm diameter particle), and μ_0 is the vacuum permeability constant (1.2566 10^{-6} H/m).

By carefully tuning the deposition time, it is possible to obtain patterns whose width is narrower than the width of the lines in the mask. This is due to the gradient of the magnetic field within the line-width defined by the mask. The magnetic field is stronger in the center than at the edges. As a result, the nanoparticles are first organized in the center of the line. The simulation of the field on the mask as a function of the distance from the mask demonstrates an interesting property of ML, as shown in figure 2.

In the present work the average magnetic field on the substrate is about 10^{-2} Tesla. Decreasing the size of the patterns, for example the width of a line, while keeping good uniformity requires using smaller particles, for example 2 nm particles. This size of particles will allow achieving line widths of about

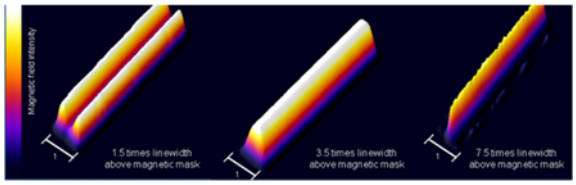

Figure 2: The magnetic field distribution above the mask, as calculated using the COMSOL program. The field distribution at distances of 1.5, 3.5, and 7.5 times the width of the mask.

20±3 nm. Assuming that the magnetic dipole of the NPs is proportional to its volume and that the gradient of the field will increase proportionally with the field, then the magnetic field required for working with 2 nm particles is about 0.1 Tesla. Such a field can be easily applied in a dedicated ML system.

Figure 3 shows the negative ML process for patterning the surface of inner tubes with enzyme and we will reveal the localization of the reaction. Here, the enzyme urease was patterned on the inside of the 500-µm diameter tube at different places using the negative ML approach.

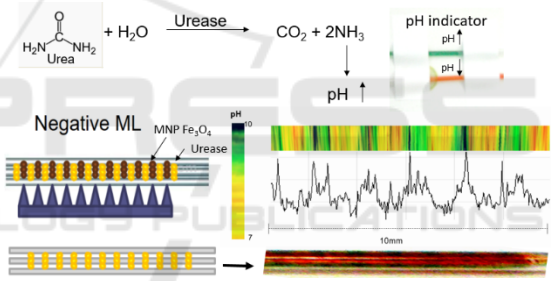

Figure 3: A scheme describing the multi-peg magnet for applying ML in the tube. The color of a pH indicator flushed in a solution of urea and pH indicator through a tube patterned with the enzyme urease. The change in pH along the tube, as obtained from the variation of the indicator's color.

The tube was exposed to a multi-peg magnet that induced a magnetic field of 100 Gauss and a solution of magnetic nanoparticles was injected into the tube. The magnetic nanoparticles were arranged along the tube according to the magnetic field induced by the magnetic pegs, as shown in Figure 3. The urease covalently bound to sites that were not protected by the magnetic NPs. A solution containing urea and a pH indicator was flown through the tube. At the regions where the urease was patterned, the enzyme decomposed the urea, producing NH_3. As a result, the pH in that region increased and the indicator changed its color to green/blue at urease binding sites. As is clearly shown in Figure 3, the high pH regions appear as green spots inside the tube. The pH variation along

the tube can be analyzed, based on the change in the color of the indicator.

A new method for DNA and RNA detection and identification using ML is presented. The detectors both DNA and RNA are determining the presence of the pathogens and their level of activity. The apply real time poly chain reaction (RT-PCR) are expensive and not portable, therefore, the proposed producing sensing device based on genomic probes inside capillary tubes will enhance the portability and the cost effectiveness of the detection process. Furthermore, the RT-PCR is mostly linear and not parallel. The new method is such RT-PCR located on top of the surface along the inner capillary tube is based on a Patterned Capillary Tube (PCT) in which the internal surface of a glass tube is patterned with rings of different single-stranded DNA probes. A solution containing the single-stranded analytes flows through the tube. Upon hybridization of appropriate DNA and RNA from the solution, DNA polymerase and reverse transcriptase (RT) are employed to synthesize the complementary nucleic acids with deoxynucleoside triphosphate (dNTP) labeled with fluorophores. The sample-analyte hybrids are detected by their fluorescence signal.

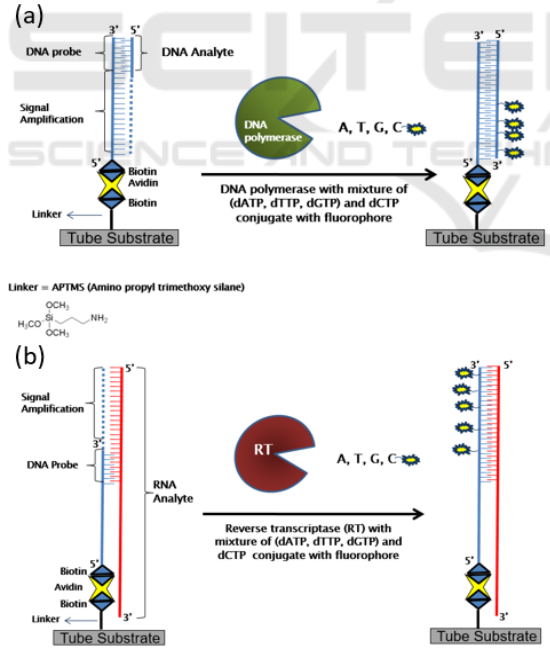

Figure 4: (a) A scheme describing the detection of DNA and amplification of the signal by using DNA polymerase and dNTPs, which include fluorescent dCTP. (b) A scheme describing the detection of RNA and amplification of the signal by using reverse transcriptase and dNTPs, which include fluorescent dCTP.

This method is sensitive, fairly simple and can detect both DNA and RNA simultaneously without pre-treatment. It is based on the ability to pattern the inner surface of a capillary tube with oligonucleotide probe molecules in well-defined locations, and subsequently flowing a solution containing the analyte DNA, RNA, or both, through the tube. Upon detection of appropriate DNA and RNA from the sample, DNA polymerase and RT are employed to synthesize the complementary nucleic acids with dNTP labeled with fluorophores (Figure 4). The formed hybrids are sensitively detected by their fluorescence signal.

The detected fluorescence signal for injection of 1µl solution containing between 10^2 to 10^{14} analyte DNA molecules (equivalent to 10^{-16} to 10^{-4} M) is shown in Figure 5. The number of molecules detected was determined by appropriate dilution of a stock solution. The signal was linear for solutions with lower than 10^5 analyte molecules and it is saturated at 10^8 molecules. The detection sensitivity to the number (rather than concentration) of molecules. Specifically, the same number of molecules was introduced into the tube, but they were dissolved in different volumes of solutions; thus the concentrations differed. The total volumes were injected into the tubes at a rate of 40 µl min-1. The signal intensity remained nearly constant, even when the solution was diluted by four orders of magnitude.

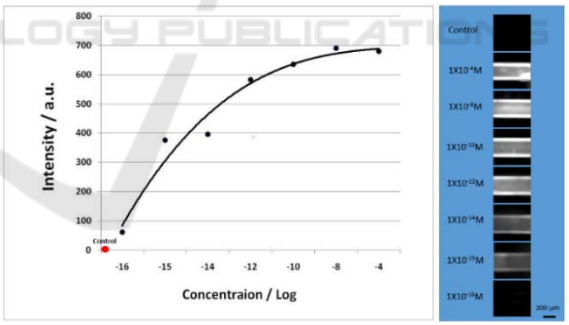

Figure 5: The fluorescence signal intensity of a DNA analyte as a function of the number of DNA molecules injected, spanning a concentration range of 12 orders of magnitude.

RNA detection was studied by designing and synthesizing a 40-base-long RNA that was used as analyte. This analyte had two sections: 1) a 3' end region of 20 bases that complement the probe (detector) sequence and 2) an additional section of a 3' end region of 20 bases which is used as a template for elongation. The second section included six guanine bases, designed to incorporate six cytosine fluorescent bases into the probe strand during RT

polymerization. Hence, six fluorescing chromophore units were bound in every analyte-probe hybridization event. The fluorescence signal obtained, as a function of the RNA analyte concentration, is shown in Figure 5. The signal spanned a range of 10 orders of magnitude in the RNA analyte concentration until reaching saturation in the presence of 10^{10} analyte molecules.

The sensitivity for native mRNA detection was tested with an 80-base-long probe, where the 20 bases at the 3' end complement N. crassa actin mRNA. A solution of 10^{-11} M (10^{7} molecules in 1 µl) total mRNA, which is within the linear response range of the device (Figure 6), was injected; the fluorescent signal saturated after 20 minutes.

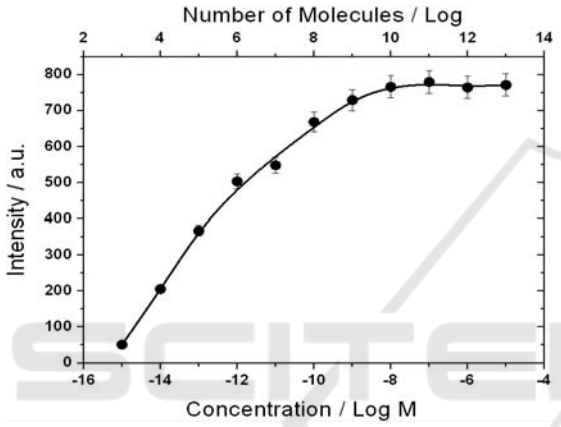

Figure 6: Concentration-dependent curve of a RNA analyte.

It is possible to use PCT without special sample preparation and to characterize both DNA and RNA from the same sample. Selectivity is obtained by appropriate design and application of the "developing solution"; to first include an enzyme that elongates one type of oligonucleotide (i.e. DNA polymerase) and subsequently injecting another developing solution that contains the enzyme required for a different elongation process (i.e. RT). This is demonstrated in Figure 7, with a tube patterned with dual-probes: one for DNA and one for RNA.

An analyte solution containing 1 pM of DNA was first injected through the tube, followed by a solution containing DNA polymerase and dNTPs. At this stage, only the DNA probe was elongated, whereas the RNA probe did not incorporate fluorescent chromophores. After injecting a solution of 1 pM RNA and addition of RT with dNTPs, the RNA probe was elongated and fluorescence was observed at the two sites. The reciprocal experiment was performed with another patterned tube and showed similar behavior.

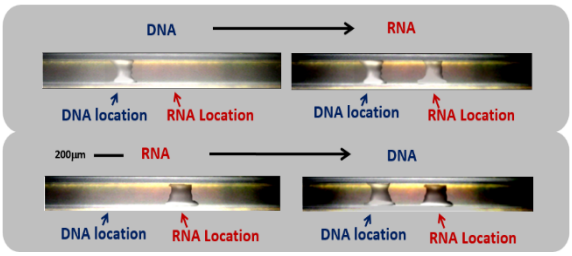

Figure 7: Demonstration of specificity and selectivity of a PCT, using a PCT patterned for both DNA and RNA detection. A DNA analyte sample was injected into the tube, followed by a "developing" solution containing DNA polymerase with dNTPs. The DNA probe site fluoresces, whereas the RNA probe site remains without signal. Following injection of RNA analyte, and a developing solution containing RT with dNTPs, the RNA site also fluoresces. A reciprocal experiment is also presented.

Here we demonstrated the ability to pattern the inside of a tube and to use the patterned substrate for sensing and catalyzing reactions in spatially localized regions. The new abilities demonstrated here open up the possibility of inducing chemical and biochemical patterning of the inner tube surfaces, especially when using tubes with a small diameter as efficient for sensitive detection and identification of DNA and RNA, lab on a chip (LOC) and for DNA sequencing.

3 CONCLUSIONS

The ML can pattern the inside of tubes by applying either positive or negative routes. The ability to pattern tubes opens up new dimensions in sensors development and applications. We report on a new ultra-sensitive and fast technique for the detection and identification of both DNA and RNA with detection sensitivity of a few molecules based on ML method. The new method is based on a Patterned Capillary Tube (PCT) in which the internal surface of a glass tube is patterned with rings of different single-stranded DNA probes using ML.

REFERENCES

Pease, R. F., Chou, S. Y. (2008) "Lithography and other patterning techniques for future electronics," Proceedings of the IEEE vol. 96, no.2, pp. 248-270.

Ito, T., Okazaki, S. (2000) "Pushing the limits of lithography," Nature vol. 406, pp. 1027-1031.

Service R. F. (2001) "EUV lithography - Optical lithography goes to extremes - and beyond," Science vol. 293, pp. 785-786.

Stewart M. E., Motala, M. J., Yao, J., Thompson, L. B., Nuzzo, R.G. (2007) "Unconventional methods for forming nanopatterns," J. Nanoengineering and Nanosystems vol. 220, pp. 81-138.

Hoeppener, S., Maoz, R., Sagiv, J (2003)"Constructive microlithography: Electrochemical printing of monolayer template patterns extends constructive nanolithography to the micrometer-millimeter dimension range," Nano Lett. vol. 3, pp. 761-767.

De Marco, C., Girardo S., Mele, E., Cingolania, R., Pisignano, D. (2008) "Ultraviolet-based bonding for perfluoropolyether low aspect-ratio microchannels and hybrid devices," Lab Chip vol. 8, pp. 1394–1397.

Li, H. W., Muir, B. V. O., Fichet, G., Huck, W. T. S (2003) "Nanocontact printing: A route to sub-50-nm-scale chemical and biological patterning," Langmuir, vol. 19, pp. 1963-1965.

McClelland, G. M. Hart, M. W. Rettner, C. T. Best, M. E. Carter, K. R. Terris, B. D. (2002) "Nanoscale patterning of magnetic islands by imprint lithography using a flexible mold," Appl. Phys. Lett. vol. 81, pp. 1483-1485.

Bandic, Z. Z. Xu, H. Hsu, Y. Albrecht, T. R. (2003) "Magnetic lithography using flexible magnetic masks: applications to servowriting," IEEE Transactions on Magnetics, vol. 39, pp. 2231-2233.

Urbach, A. R. J. Love, C. Prentiss, M. G. Whitesides, G. M. (2003)"Sub-100 nm confinement of magnetic nanoparticles using localized, magnetic field gradients," JACS, vol. 125, pp. 12704-12705.

Bardea A., Naaman, R. (2009) "Magnetolithography: From Bottom-Up Route to High Throughput," Small, vol. 5, pp. 316-319.

Bardea A. Yoffe, A. (2017) "Magneto-Lithography, a simple and inexpensive method for high throughput, surface patterning,", IEEE Trans. on Nanotechnology, vol. 16, no. 3, pp. 439-444.

Bardea A. (2018)“Novel approach of backside lithography using dynamic magnetic mask” Int'l. Conf. on the Science of Electrical Engineering (ICSEE).